Cycle-to-cycle variations in cross-flow turbine performance and flow fields: *Experiments in Fluids Supplementary Material*

Abigale Snortland[*1], Isabel Scherl[1], Brian Polagye[1], Owen Williams[2]

July 22, 2024

[*]Corresponding author email: abigales@uw.edu
Contributing authors email: ischerl@uw.edu, bpolagye@uw.edu, ojhw@uw.edu
[*1]University of Washington, Mechanical Engineering, 3900 E Stevens Way NE, Seattle, WA 98195, USA
[2]University of Washington, Aeronautics and Astronautics, 3940 Benton Lane NE, Seattle, WA 98195, USA

For brevity, the main body of the paper focuses on the clustering result from flow-field segment S_b. Here we present a comparison of the clustering results for all of the flow-field segments, S_a-S_e. Figures 1-5 summarize the comparison of the flow-field clusters for segments S_a-S_e and their corresponding performance trajectories for the two tip-speed ratios. As in the main body, we designate cluster 1 as the cluster with higher time-averaged performance. The conditionally-averaged difference fields (panels i and ii) highlight the deviation between the cluster conditionally-averaged flow fields and the phase-averaged fields (iii). The performance trajectories (iv) and their perturbations from the phase-average (v) for each cycle reveal connections between performance and the flow-field clusters.
Across all segments and for both tip-speed ratios, the conditionally-averaged difference fields reveal opposing behaviors between the clusters (e.g., regions of lower-than-average relative velocities in one cluster are coincident with regions of higher-than-average relative velocities in the other). The differences are more pronounced for $\lambda = 1.5$ than for $\lambda = 2.5$. Yet, for both tip-speed ratios, performance trajectories are separated by their associated flow-field clusters and exhibit opposing behaviors around the phase average. Notably, the flow-field clusters for both tip-speed ratios are associated with differences in maximum performance within a cycle, even for clusters derived from flow segments in the downstream sweep. This shows that flow fields throughout the rotation have ties to performance.

The differences between the performance trajectories associated with the flow-field clusters are summarized in Figure 6. The difference between the time-averaged performance of the two clusters relative to the time-average of all cycles in a given segment (Figure 6a) is highest for S_a suggesting the strongest correlation between the flow fields and performance is found here. This is notable, given that the differences between the conditionally-averaged flow fields are relatively subtle (Figure 1). In comparison, the differences in time-averaged performance between the clusters are lower for but consistent across all other segments (S_b-S_e). The difference between phase-averaged performance for the two clusters is shown in Figure 6b. For both tip-speed ratios, the difference in performance in the upstream sweep depends on the flow segment while differences in the downstream sweep are relatively insensitive to the flow segment. For flow-field clusters based on segments in the downstream sweep for $\lambda = 1.5$, the difference between the two cluster's performance is reduced at the phases of maximum and minimum performance, compared to S_a-S_b (i.e., the difference at $\theta = 90°$ is greater for S_a than S_d). This is expected, since in the downstream sweep, the hydrodynamic features associated with power production at the peak advect, diffuse, and are diluted in the complex post-stall region, thereby obscuring their connection to the hydrodynamic mechanisms driving performance variability earlier in the cycle. For $\lambda = 2.5$, the amount of variation in maximum performance between the two clusters is similar for segments S_b and S_e. This is likely because the hydrodynamics in the downstream sweep are less complex in comparison to $\lambda = 1.5$, and variations in the downstream sweep are

likely associated with the same hydrodynamic mechanisms that contribute to the performance variability in the upstream sweep. Overall, despite the apparent mismatch in flow-field and performance variability in the downstream sweep for both tip-speed ratios (Figure 9 in the paper), the flow-field clusters for segments in the downstream sweep are still closely connected with time and phase-averaged performance.

The singular values for the five different data matricies ($A_{\#}$) are presented in Figure 7. As part of determining the location of the dynamic stall vortex in the paper, the flow fields are reconstructed with 30 modes. By this point, the singular values are small, and the dominant vortex dynamics are retained in the truncation.

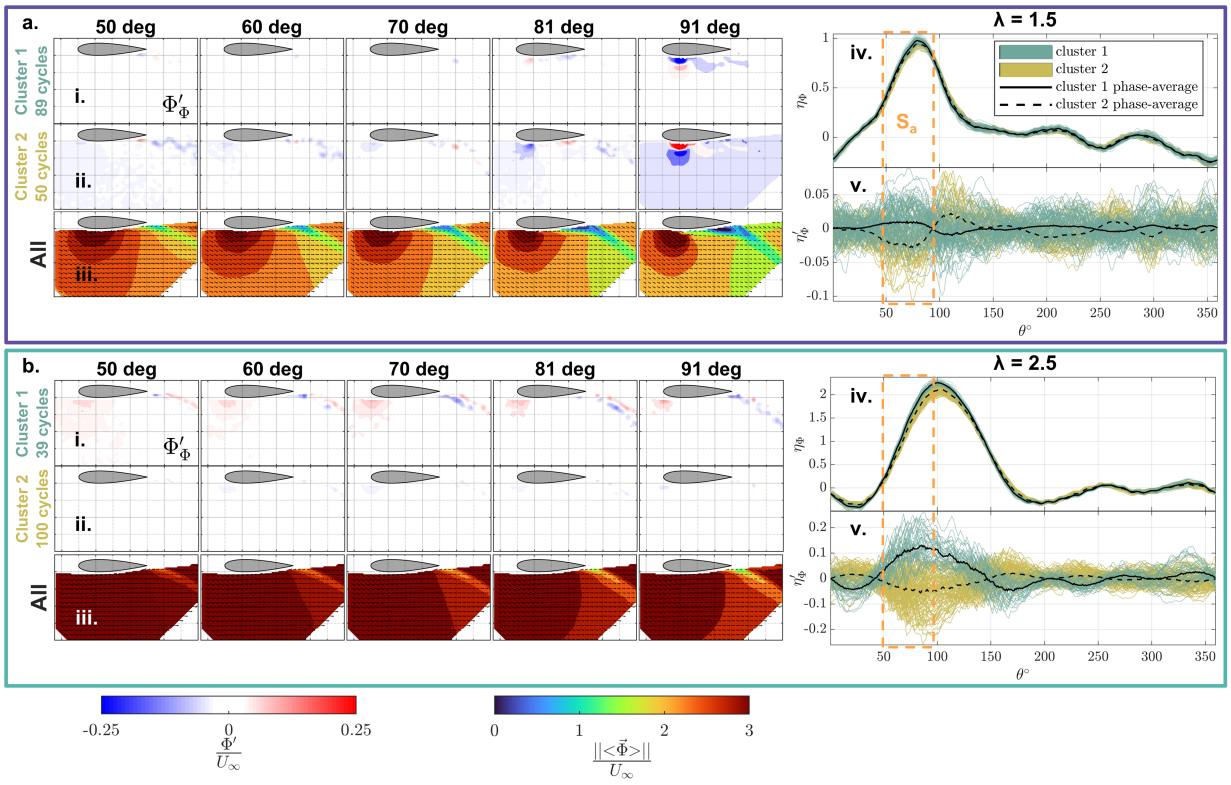

Figure 1: Clustering analysis overview for for (a) $\lambda = 1.5$ (b) and $\lambda = 2.5$. (i,ii) Cluster conditional difference flow fields and (iii) phase averages for selected θ, with (iv) corresponding performance trajectories and (v) performance perturbations. The grid spacing in (i), (ii) and (iii) is $C/4$. In (iv), each line is colored by cluster assignment and the black lines represent the cluster conditional-averages for performance or performance perturbations. The dashed rectangles denote the θ range (S_a) where the flow fields in (i),(ii) and (iii) were captured.

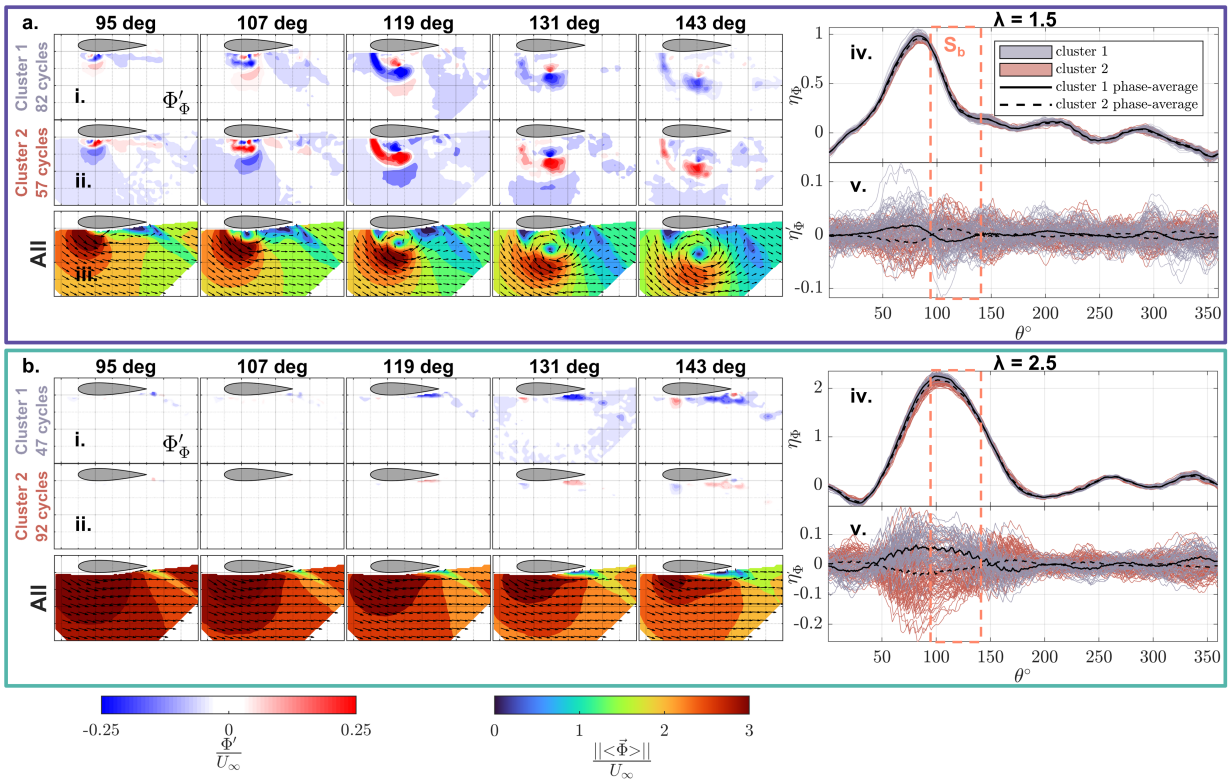

Figure 2: Clustering analysis overview for for (a) $\lambda = 1.5$ (b) and $\lambda = 2.5$. (i,ii) Cluster conditional difference flow fields and (iii) phase averages for selected θ, with (iv) corresponding performance trajectories and (v) performance perturbations. The grid spacing in (i), (ii) and (iii) is $C/4$. In (iv), each line is colored by cluster assignment and the black lines represent the cluster conditional-averages for performance or performance perturbations. The dashed rectangles denote the θ range (S_b) where the flow fields in (i),(ii) and (iii) were captured.

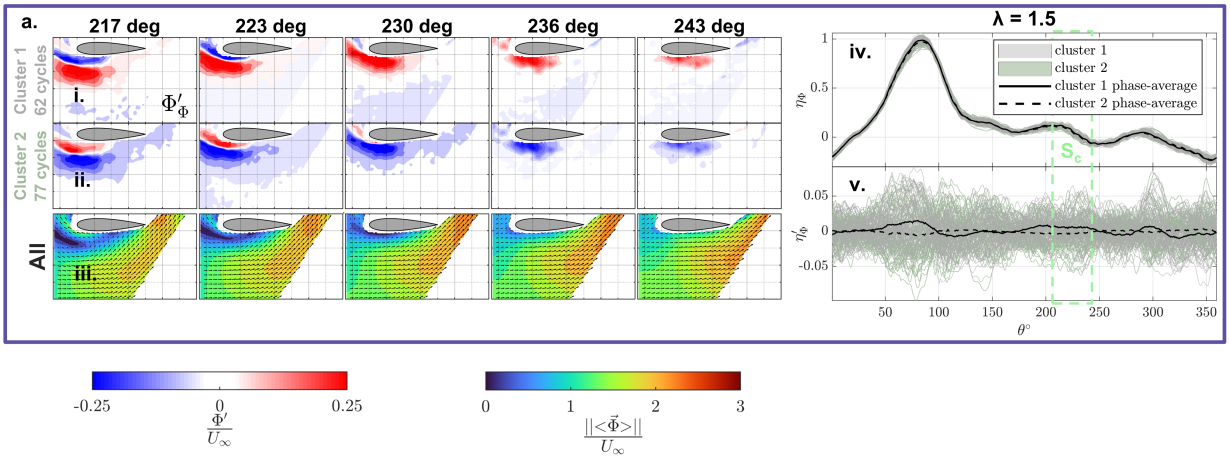

Figure 3: Clustering analysis overview for for (a) $\lambda = 1.5$. No flow field information was captured for this segment at $\lambda = 2.5$. (i,ii) Cluster conditional difference flow fields and (iii) phase averages for selected θ, with (iv) corresponding performance trajectories and (v) performance perturbations. The grid spacing in (i), (ii) and (iii) is $C/4$. In (iv), each line is colored by cluster assignment and the black lines represent the cluster conditional-averages for performance or performance perturbations. The dashed rectangles denote the θ range (S_c) where the flow fields in (i),(ii) and (iii) were captured.

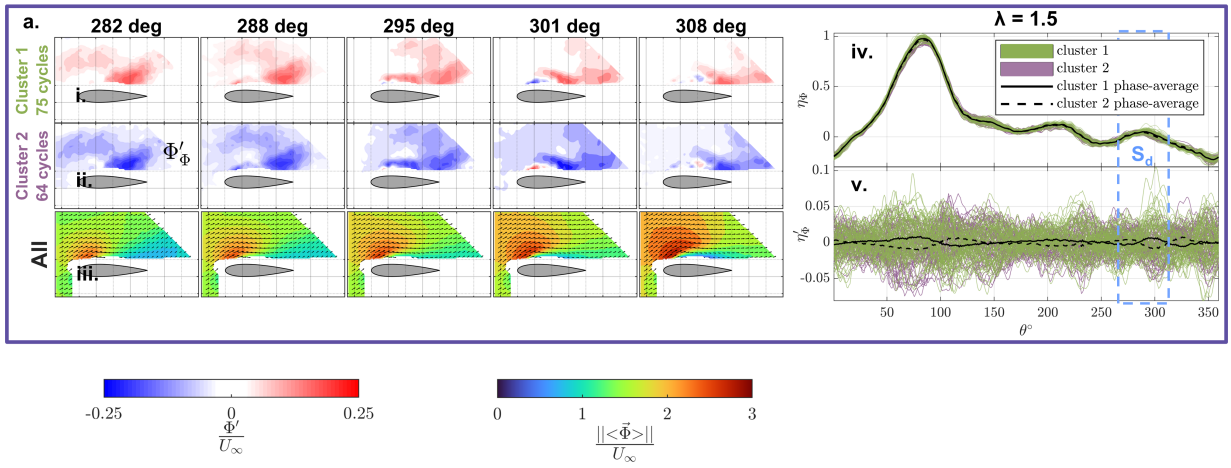

Figure 4: Clustering analysis overview for for (a) $\lambda = 1.5$. No flow field information was captured for this segment at $\lambda = 2.5$. (i,ii) Cluster conditional difference flow fields and (iii) phase averages for selected θ, with (iv) corresponding performance trajectories and (v) performance perturbations. The grid spacing in (i), (ii) and (iii) is $C/4$. In (iv), each line is colored by cluster assignment and the black lines represent the cluster conditional-averages for performance or performance perturbations. The dashed rectangles denote the θ range (S_d) where the flow fields in (i),(ii) and (iii) were captured.

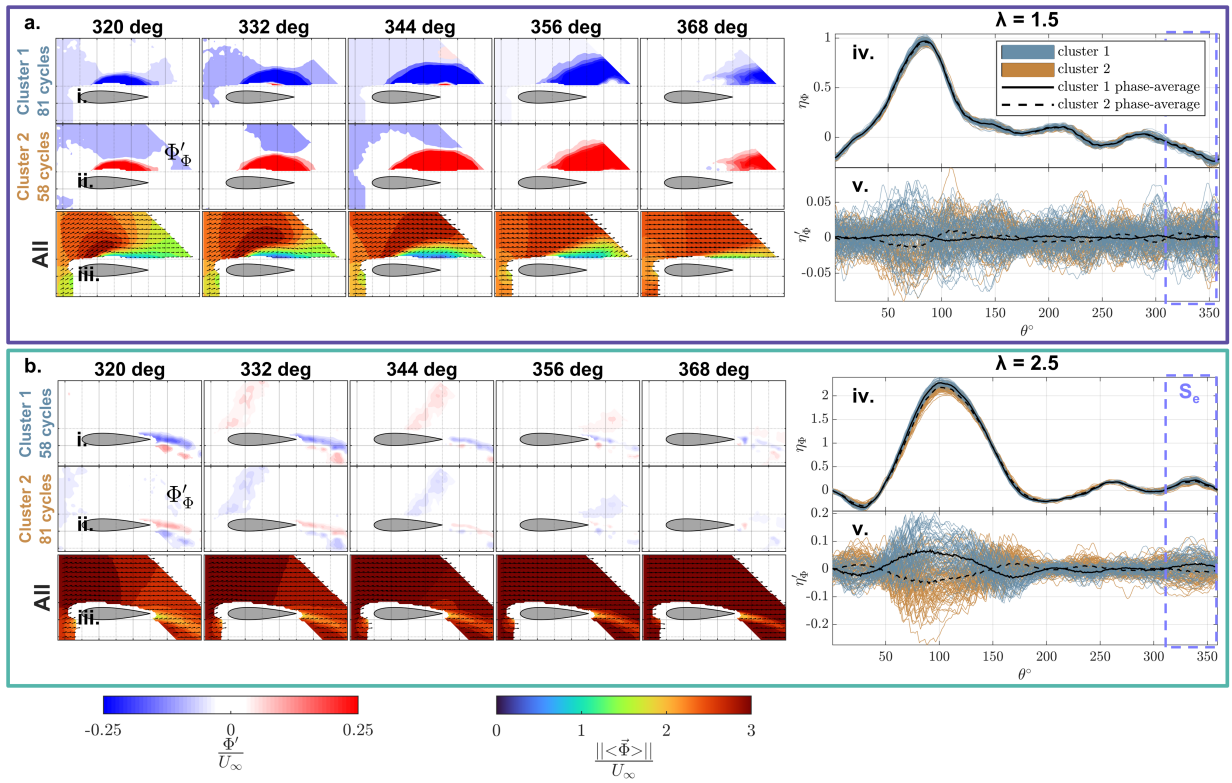

Figure 5: Clustering analysis overview for for (a) $\lambda = 1.5$ (b) and $\lambda = 2.5$. (i,ii) Cluster conditional difference fields and (iii) phase averages for selected θ, with (iv) corresponding performance trajectories and (v) performance perturbations. The grid spacing in (i), (ii) and (iii) is $C/4$. In (iv), each line is colored by cluster assignment and the black lines represent the cluster conditional-averages for performance or performance perturbations. The dashed rectangles denote the θ range (S_e) where the flow fields in (i),(ii) and (iii) were captured.

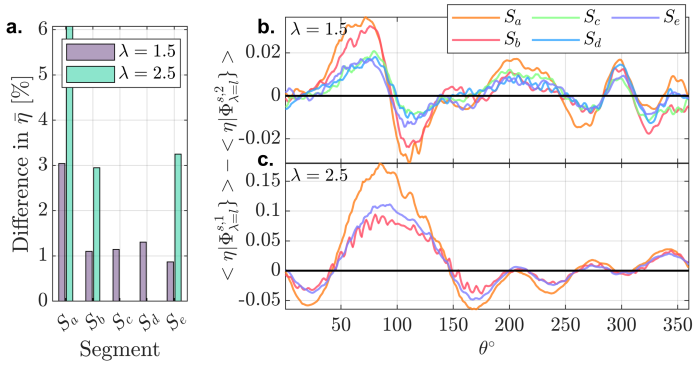

Figure 6: Clustering analysis comparison between all flow segments. (a) Percent differences in time-averaged performance between the clusters with respect to time-averaged performance of all cycles. (b,c) Difference in phase-averaged performance between the clusters for (b) $\lambda = 1.5$ (c) and $\lambda = 2.5$.

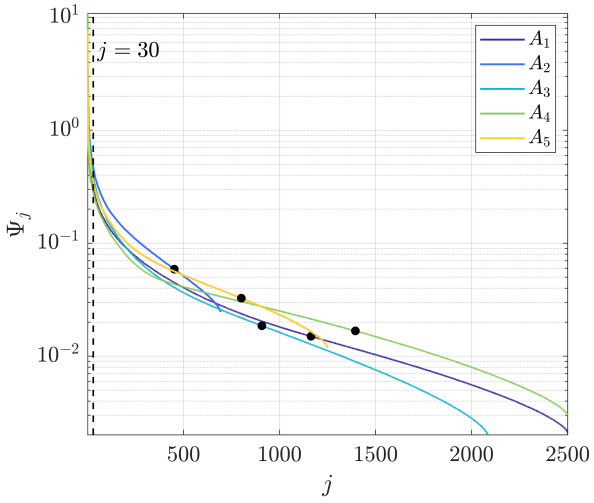

Figure 7: Singular values for the five different data matrices ($A_\#$). The black dots denote the mode at which 90% of the variance is explained. The dashed line denotes 30 modes which is where the data is truncated for vortex tracking.